

# Thermal conductivity of epitaxial graphene nanoribbons on SiC

Zhi-Xin Guo<sup>1\*</sup>, J. W. Ding<sup>1</sup> and Xin-Gao Gong<sup>2</sup>

<sup>1</sup>Department of Physics, Xiangtan University, Xiangtan, Hunan 411105, China

<sup>2</sup>Surface Physics Laboratory and Department of Physics, Fudan University, Shanghai 200433, China\*

(Dated: November 2, 2019)

We investigate thermal conductivity of epitaxial single-layer and bilayer graphene nanoribbons (GNRs) on SiC substrate using the nonequilibrium molecular dynamics method. Both covalently bonded and weakly coupled GNR-substrate interaction conditions are considered. In the covalently bonded condition, the thermal conductivity of single-layer GNRs is particularly low, while, in the weakly coupled condition the thermal conductivity is close to that of the suspended GNRs. The second GNR layer in a bilayer GNR is found to have the highest thermal conductivity among all the epitaxial GNRs, which also keeps much the same thermal conductivity characteristics as the suspended GNRs. We further find the out-of-plane phonon mode plays a critical role on the thermal conductivity reduction of the second GNR layer.

PACS numbers:

Graphene and Graphene nanoribbon (GNR) are thought to be ideal materials for nanoelectronics due to their outstanding electronic and thermal properties[1–6]. In the production, the graphene nanomaterials can be either prepared by mechanical exfoliation from graphite[7, 8] or by epitaxial growth on SiC substrate[9, 10]. However, the mechanical method is quite delicate and time consuming, which makes it unapplicable in the industry. The epitaxial growth method is nowadays commonly accepted to represent a viable method of controllable growth for the fabrication of high quality graphene wafers[11]. The electronic properties of epitaxial graphene on SiC substrate had been extensively studied[10, 12–14]. It was found the electronic properties of graphene can be well preserved in both the single-layer (SL) graphene on SiC (0001) (C-terminated)[10], and the second layer of bilayer (BL) graphene on SiC(0001)(Si-terminated)[12, 13], implying great application potential of epitaxial graphene in the nanoelectronics. Since the heat removal is a crucial issue in the nanoelectronic industry, the thermal conduction property of epitaxial graphene and GNR becomes particularly important to its application in the nanoelectronics.

During the last two years, the thermal conductivity of exfoliated graphene on different substrates (SiO<sub>2</sub>, Cu) has been extensively studied, where only weakly coupled graphene-substrate interaction exists[15–19]. Different from the exfoliated graphene case, the epitaxial graphene-substrate interaction is much more complicated, and the geometry can even be distorted by the substrate [12, 20]. Thus the thermal conductivity of epitaxial graphene and GNR is expected to be very different from the exfoliated ones.

In this work, we use the nonequilibrium molecular dynamics (NEMD)[6, 21–23] method to study the thermal conductivity of epitaxial GNRs on 4H-SiC (0001) and

(0001) surface. On the (0001) surface, both covalently bonded and weakly coupled GNR-substrate interaction conditions that were observed by the experiments are considered. On the (0001) surface, we consider both the SL and BL GNR-substrate interaction cases. In the BL GNR, we concentrate on the thermal conductivity of the second layer since the first layer is expected to have similar thermal conductivity as the SL GNR. Two typical GNRs, i.e., armchair GNR (AGNR) and zigzag GNR (ZGNR), are considered, and we refer to AGNR/ZGNR with N dimer lines in width as N-AGNR/N-ZGNR for convenient representation[24].

The 4H-SiC substrate is modeled with four alternating Si and C atomic layers. One Si-C layer at the bottom of the sample is fixed. GNRs are placed on top of the SiC substrate, with infinite length along the X direction and finite width along Y direction. The smallest cell of the GNR-SiC system is of 10.12 nm in length (X direction) and 2.15 nm (around 1 nm) for the SiC (GNR) in width (Y direction), containing 2128 SiC atoms and 320 (368) 4-ZGNR (8-AGNR) atoms, respectively.

In the geometry optimization, periodic boundary conditions are applied both along the X and Y directions. We use the Tersoff[25] potential to describe the C-C and C-Si bonded interactions, and the non-bonded van der Waals interaction is described by the Lennard-Jones (LJ) potential[26], which is only nonzero after the Tersoff covalent potential goes to zero. The coupling between the long-range LJ potential and the short-range Tersoff potential is described by a cubic spline function[27].

In the NEMD simulation, we employ the velocity Verlet method to integrate equations of motion with a fixed time step of 1 fs. Fixed boundary condition is applied along the X direction, where the outmost layers of each end of GNR (SiC) are fixed. Next to the boundaries, the adjacent 1 nm-long GNR (SiC) layers are coupled to the Nosé-Hoover[28] thermostats with temperatures 310 and 290 K, respectively. The thermal conductivity of GNRs

\*Electronic address: zxguo08@gmail.com

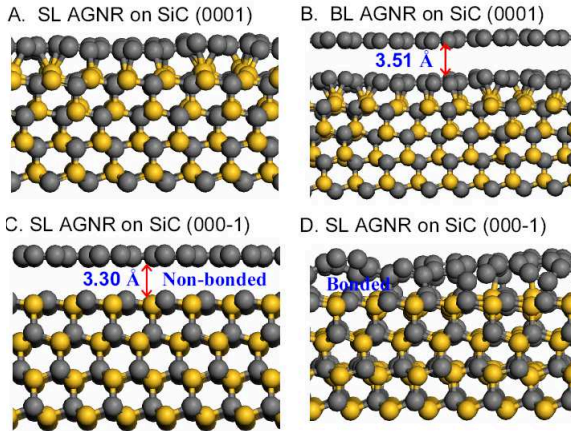


FIG. 1: Optimized structures of the 8-AGNR on SiC substrate for 4 cases: A, single-layer GNR on SiC (0001); B, bi-layer GNR on SiC (0001); C, single-layer GNR on SiC (000 $\bar{1}$ ) with weakly coupled interaction; D, single-layer GNR on SiC (000 $\bar{1}$ ) with covalently bonded interaction. Carbon atoms are represented by gray balls; Si, by yellow balls.

$\kappa$  is then calculated from the Fourier law,

$$\kappa = -\frac{J}{\nabla T \cdot S}, \quad (1)$$

where  $J$  is the heat flux from the thermostats to the system, which is obtained from the Green-Kubo relation[29, 30].  $\nabla T$  is the temperature gradient in the length direction, which is defined as  $\nabla T = (T_L - T_R)/L$ , where  $T_L$ ,  $T_R$  are the temperature of thermostats at the two ends, and  $L$  is GNR length.  $S$  is the cross-section area. In this work, we choose the interplanar spacing of graphite 3.35 Å as the GNRs' thickness. Moreover, all results given in this paper are obtained by averaging about 5 ns after a sufficient long transient time (5 ns) when a nonequilibrium stationary state is set up.

The following 4 kinds of epitaxial GNRs on SiC are considered: A, SL GNR on SiC (0001); B, BL GNR on SiC(0001); C, SL GNR on SiC (000 $\bar{1}$ ) with the weakly coupled interaction; D, SL GNR on SiC (000 $\bar{1}$ ) with the covalently bonded interaction. Before geometry optimization, the initial distance between GNR and SiC surface was set to be 2.3 Å in cases A and B, 3.0 Å in case C, and 2.0 Å in case D. In Fig. 1, we show the optimized structures of 8-AGNR on SiC for the above 4 cases. As one can see, the SL GNRs can either covalently bonded or weakly coupled to the substrate. In the covalently bonded case (case A, D), the formed C-Si (C-C) covalent bond between GNR and substrate has a length around 2.15 (1.60) Å in the middle region, being consistent with the bond length of the graphene-SiC system in previous reports [12, 13, 31]. While, in the edge region the C-Si (C-C) bond length is only about 2.10 (1.50) Å, shorter than that in the middle region, indicating that the edge atoms make the interaction between GNR and substrate

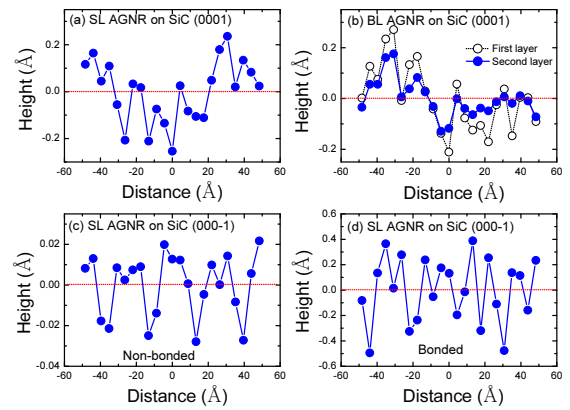


FIG. 2: The height profile of GNRs on SiC along the length direction for cases A (a), B (b), C (c), and D (d).

stronger than that between graphene and substrate. In the weakly coupled case (case C), the mean distance between GNR and SiC surface is 3.30 Å, similar with the graphene case[32].

In the BL GNR (case B), while, the mean distance between the first and the second layer is 3.51 Å, obviously larger than the interlayer distance of the suspended BL graphene. The larger interlayer distance comes from the larger shear modules of GNRs[33] and the large ripples formed on first GNR layer due to its strong interaction with SiC surface[34]. Compared with the BL graphene, the interlayer force in BL GNR is smaller due to its finite width, while its shear modules is much larger. Thus, unlike the BL graphene, the weak interlayer van der Walls force can't make the second GNR layer follows the large ripples of the first GNR layer, and the second GNR layer still keeps a relatively planar structure. The large interlayer distance appears at the trough of the ripple in first GNR layer.

The corresponding height profile of GNRs on SiC along the length direction is shown in Fig. 2. From the figure, the ripples of GNRs that covalently bonded with SiC are obviously larger than that of GNRs weakly coupled with SiC. The smallest and largest ripples appear in case C and D, respectively, both of which are on SiC (000 $\bar{1}$ ). Moreover, in the BL GNR the ripple of the second GNR layer is obviously smaller than that of first GNR layer (Fig. 2(b)), which corresponds to a larger interlayer distance as discussed above.

Fig. 3 shows the width dependence of thermal conductivity of both AGNRs and ZGNRs on SiC. As shown in the figure, the thermal conductivity of GNRs covalently bonded with SiC is very different from that weakly coupled with SiC. In the covalently bonded case, thermal conductivity of GNRs is very low (below 30 W/mK), and has little variation when the width gets larger than 2 nm. This shows that the strong covalent Si-C/C-C bonds formed between GNR and SiC surface have destroyed the intrinsic thermal conductivity of GNRs. In addition, the

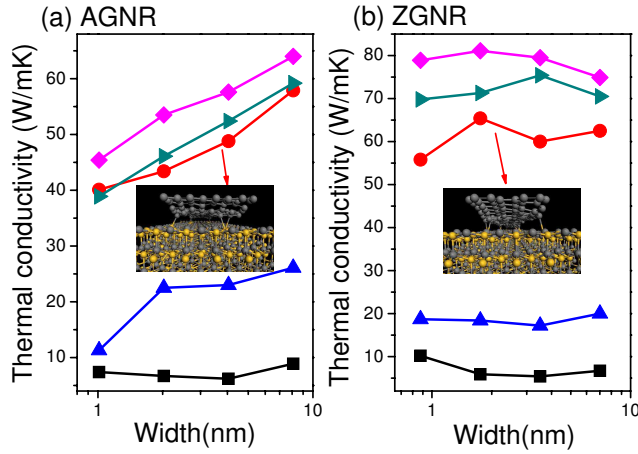


FIG. 3: Width dependence of thermal conductivity of both AGNRs (a) and ZGNRs (b) on SiC in cases A (blue uptriangle), B (cyan righttriangle), C (red circle), and D (black square), with comparison of the suspended GNRs (magenta diamond). In cases A, D the thermal conductivity of epitaxial GNR is particularly low, while, in cases B, C the thermal conductivity is close to that of the suspended GNR.

thermal conductivity of GNR on SiC (0001) (case D) is distinctly smaller than that on the (0001) surface (case A). This is attributed to the larger GNR ripples formed on the (0001) surface than that on (0001) surface (see Fig. 2), which would induce stronger phonon scattering.

Different from the covalently bonded case, thermal conductivity of GNRs weakly coupled with SiC is much higher (case B, C), being close to that of the suspended GNRs. The width-dependence of thermal conductivity is also similar with the suspended GNRs: With the width increasing, the thermal conductivity of AGNR monotonously increases, while the thermal conductivity of ZGNR increases first and then decreases[6]. This implies the weakly coupled interaction does not destroy the intrinsic thermal conductivity of GNRs. Moreover, the thermal conductivity of the second layer of BL GNR on SiC(0001) (case B) is even higher than that of the SL GNR on SiC(0001) (case C). This is attributed to two facts. On one hand, the interlayer distance (4.51 Å) of BL GNR on SiC(0001) is larger than the distance (3.30 Å) between SL GNR and SiC (0001). Thus the phonon scattering from substrate is stronger in the SL GNR than that in the BL GNR. On the other hand, some C-Si covalent bonds are newly formed between the edge of SL GNR and SiC(0001) surface when the system is thermostated to 300 K (inset of Fig. 3), owing to the big amplitude of GNR perpendicular to the surface. This would also induce additional edge localized phonon scattering on the GNR, and thus the thermal conductivity is further reduced.

From above results, it is definite that the second GNR layer of BL GNR on SiC has the highest thermal conductivity among all the epitaxial GNRs. In Fig. 4 we show

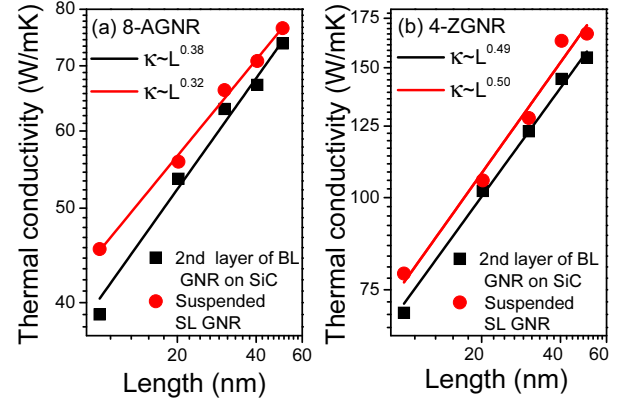


FIG. 4: Length dependence of thermal conductivity of the second 8-AGNR (a), 4-ZGNR (b) layers in BL GNR with comparison of the suspended GNRs. Thermal conductivity of the second GNR layers monotonously increases with the length increasing and follows a power law of  $\kappa \sim L^\beta$ , with  $\beta$  being close to that of the suspended GNRs.

TABLE I: Thermal conductivity ( $\kappa$ ) of the 8-ZGNR with and without the out-of-plane vibrational constraint. The GNR length is kept at 10 nm.

GNR type	Constraint	$\kappa$ (W/mK)
SL GNR	Free	81.1
SL GNR	Constraint	77.7
2nd layer of BL GNR	Free	71.3
2nd layer of BL GNR	Constraint	79.1

the length dependence of thermal conductivity of the second GNR layer of BL GNR with comparison of the suspended GNR. Similar with that of the suspended GNRs and carbon nanotubes[6, 35], the thermal conductivity of the second 8-AGNR (4-ZGNR) layer monotonously increases with the length increasing and follows a power law of  $\kappa \sim L^\beta$ , with  $\beta=0.38$  (0.49). The value of  $\beta$  is very close to that of the suspended GNR ( $\beta=0.32$  (0.50)), showing that the ballistic and 1D thermal transport characters[35–37] are well preserved in the second GNR layer.

To further explore the substrate effect on thermal conductivity of the second GNR layer of BL GNR on SiC, we freeze the out-of-plane atomic vibration of the second GNR layer and recalculate the thermal conductivity with comparison of the suspended SL GNR. For simplicity, here we only present the calculated thermal conductivity of the ZGNRs, the results of the AGNRs are similar. As shown in Table 1, freezing the out-of-plane atomic vibration would decrease the thermal conductivity of the suspended SL GNR, while considerably increase the thermal conductivity of the second GNR layer of BL GNR.

This illustrates two facts. One is that the out-of-plane phonon mode in suspended SL GNR has a positive contribution to the thermal transport, although the contri-

bution is not dominating. The other is that the thermal conductivity reduction of the second GNR layer of BL GNR mainly comes from the coupling between its out-of-plane phonon mode and the phonon modes of the substrate (including phonon modes of both first GNR layer[38] and SiC surface). It should be mentioned that, the thermal conductivity of the second GNR layer (79.1 W/mK) in BL GNR is even higher than that of the suspended SL GNR (77.7 W/mK) when the out-of-plane atomic vibration is frozen. This interesting phenomenon indicates an increment of thermal conductivity can be realized through the substrate coupling without the out-of-plane phonon coupling. Recently, through a coupled atomic chain model, we have clarified that there exists a competitive mechanism on thermal conductivity in a coupling system: the phonon resonance effect that decreases thermal conductivity and phonon-band-up-shift effect that increases thermal conductivity[23]. In this case, the phonon resonance effect mainly comes from the coupling between out-of-plane phonon mode of the second GNR layer and the phonon modes of the first GNR layer and substrate. When the out-of-plane atomic vibration is frozen, the phonon resonance effect would be largely reduced, and the phonon-band-up-shift effect become dominated. Thus the thermal conductivity can be increased by the coupling. The results further confirm the existence of two competitive effects between thermal

conductive material and substrate.

In summary, we have investigated the thermal conductivity of epitaxial SL and BL GNRs on SiC substrate using the nonequilibrium molecular dynamics method. Both covalently bonded and weakly coupled GNR-substrate interaction conditions are considered. In the covalently bonded condition, the thermal conductivity of SL GNRs is particularly low and has different width-dependence behavior with the suspended GNRs. In the weakly coupled condition, the thermal conductivity of GNRs is much higher and exhibits similar width-dependence as that of the suspended GNRs. The second GNR layer of BL GNRs is found to have the highest thermal conductivity among all the epitaxial GNRs, and keeps much the same thermal conductivity characteristics as the suspended GNRs. Through a constraint simulation, we find that the out-of-plane phonon mode in the second GNR layer plays a critical role on the thermal conductivity reduction. The existence of two competitive effects between thermal conductive material and substrate is further confirmed. We expect the present study can be helpful to the forthcoming applications of epitaxial graphene nanomaterials in the nanoelectronics.

This work is supported by Start-up funds (No. 10QDZ11) and Scientific Research Fund (10XZX05) of Xiangtan University.

---

[1] A. K. Geim, *Science* 324, 1530 (2009).  
[2] A. H. Castro Neto, F. Guinea, N. M. R. Peres, K. S. Novoselov, and A. K. Geim, *Rev. Mod. Phys.* 81, 109 (2009).  
[3] A. A. Balandin, S. Ghosh, W. Bao, I. Calizo, D. Teweldebrhan, F. Miao, and C. N. Lau, *Nano Lett.* 8, 902 (2008).  
[4] A. A. Balandin, *Nature Mater.* 10, 569 (2011).  
[5] J. Hu, X. Ruan, and Y. P. Chen, *Nano Lett.* 9, 2730 (2009).  
[6] Z. X. Guo, D. Zhang, and X. G. Gong, *Appl. Phys. Lett.* 95, 163103 (2009).  
[7] K. S. Novoselov, A. K. Geim, S. V. Morozov, D. Jiang, M. I. Katsnelson, I. V. Grigorieva, S. V. Dubonos, and A. A. Firsov, *Nature* 438, 197 (2005).  
[8] Y. Zhang, Y. W. Tan, H. L. Stormer, and P. Kim, *Nature* 438, 201 (2005).  
[9] W. A. de Heer, C. Berger, X. S. Wu, P. N. First, E. H. Conrad, X. B. Li, T. B. Li, M. Sprinkle, J. Hass, M. L. Sadowski, M. Potemski, and G. Martinez, *Solid State Commun.* 143, 92 (2007).  
[10] K. V. Emtsev, F. Speck, T. Seyller, L. Ley, and J. D. Riley, *Phys. Rev. B* 77, 155303 (2008).  
[11] C. Dimitrakopoulos, Y. M. Lin, A. Grill, D. B. Farmer, M. Freitag, Y. Sun, S. J. Han, Z. Chen, K. A. Jenkins, Y. Zhu, Z. Liu, T. J. McArdle, J. A. Ott, R. Wisnieff, and P. Avouris, *J. Vac. Sci. Technol. B* 28, 985 (2010).  
[12] A. Mattausch, and O. Pankratov, *Phys. Rev. Lett.* 99, 076802 (2007).  
[13] F. Varchon, R. Feng, J. Hass, X. Li, B. NgocNguyen, C. Naud, P. Mallet, J. Y. Veuillen, C. Berger, E. H. Conrad, and L. Magaud, *Phys. Rev. Lett.* 99, 126805 (2007).  
[14] S. Kim, J. Ihm, H. J. Choi, and Y. W. Son, *Phys. Rev. Lett.* 100, 176802 (2008).  
[15] J. H. Seol, I. Jo, A. L. Moore, L. Lindsay, Z. H. Aitken, M. T. Pettes, X. Li, Z. Yao, R. Huang, D. A. Broido, N. Mingo, R. S. Ruoff, and L. Shi, *Science* 328, 213 (2010).  
[16] W. Jang, Z. Chen, W. Bao, C. N. Lau, and C. Dames, *Nano Lett.* 10, 3909 (2010).  
[17] Y. K. Koh, M. H. Bae, D. G. Cahill, and E. Pop, *Nano Lett.* 10, 4363 (2010).  
[18] Z. Wang, R. Xie, C. T. Bui, D. Liu, X. Ni, B. Li, and T. L. J. Thong, *Nano Lett.* 11, 113 (2011).  
[19] Z. Y. Ong, and E. Pop, *Phys. Rev. B* 84, 075471 (2011).  
[20] V. Sorkin, and Y. W. Zhang, *Phys. Rev. B* 81, 085435 (2010).  
[21] Z. X. Guo, D. Zhang, Y. T. Zhai, and X. G. Gong, *Nanotechnology* 21, 285706 (2010).  
[22] Z. X. Guo, and X. G. Gong, *Front. Phys.* 4, 389 (2009).  
[23] Z. X. Guo, D. Zhang, and X. G. Gong, *Phys. Rev. B* 84, 075470 (2011).  
[24] Y. W. Son, M. L. Cohen, and S. G. Louie, *Phys. Rev. Lett.* 97, 216803 (2006).  
[25] J. Tersoff, *Phys. Rev. B* 39, 5566 (1989).  
[26] L. A. Girifalco, M. Hodak, and R. S. Lee, *Phys. Rev. B* 62, 13104 (2000).  
[27] Z. Mao, A. Garg, and S. B. Sinnott, *Nanotechnology* 10, 273 (1999).  
[28] S. Nosé, *J. Chem. Phys.* 81, 511 (1984); W. G. Hoover, *Phys. Rev. A* 31, 1695 (1985).  
[29] P. K. Schelling, S. R. Phillpot, and P. Kebinski *Phys.*

Rev. B 65, 144306 (2002).

[30] N. Yang, G. Zhang, and B. Li, Nano Lett. 8, 276 (2008).

[31] Y. Qi, S. H. Rhim, G. F. Sun, M. Weinert, and L. Li, Phys. Rev. Lett. 105, 085502 (2010).

[32] F. Hiebel, P. Mallet, J. Y. Veuillen, and L. Magaud, Phys. Rev. B 83, 075438 (2011).

[33] R. Faccio, P. A. Denis, H. Pardo, C. Goyenola, and Á. W. Mombrú, J. Phys.: Condens. Matter 21, 285304 (2009).

[34] F. Varchon, P. Mallet, J. Y. Veuillen, and L. Magaud, Phys. Rev. B 77, 235412 (2008).

[35] S. Maruyama, Physica B 323, 193 (2002).

[36] E. Enrique, J. Lu, and B. I. Yakobson, Nano Lett. 10, 1652 (2010).

[37] G. Zhang, and B. Li, J. Chem. Phys. 123, 114714 (2005).

[38] H. Y. Cao, Z. X. Guo, H. J. Xiang, and X. G. Gong, Phys. Lett. A 376, 525 (2012).